Materials Today Communications 31 (2022) 103469

Contents lists available at ScienceDirect

Materials Today Communications

journal homepage: www.elsevier.com/locate/mtcomm

Synthesis of high thermal stability Polypropylene copolymers with pyrrole functionality

Rosana Vaquero-Bermejo, Enrique Blázquez-Blázquez [1], Mario Hoyos [2], José M. Gómez-Elvira [*,3]

Instituto de Ciencia y Tecnología de Polímeros (ICTP), Consejo Superior de Investigaciones Científicas (CSIC), Juan de la Cierva, 3, 28006 Madrid, Spain

ARTICLE INFO

Keywords:
Functional polyolefins
Reactive polypropylene
Cross-linked polypropylene
High thermal stability polypropylene

ABSTRACT

Functionalization of polyolefins has been proven to be a promising way to fine-tune their properties, among which, improved thermal stability is crucial for high performance in end-use applications. However, it still remains in academia, as some important issues still need to be resolved for this methodology to move towards industrial scale-up, the most important of them being the development of one-step processes. This work focuses specifically on the development of a single-step functionalization route for the synthesis of high thermal and thermo-oxidative stability polypropylenes. The synthesis of Polypropylene (PP) bearing N-alkyl groups by copolymerization via metallocene catalysis is studied. The copolymers are found to exhibit high thermo-oxidative stability, whose origin appears to be based, not only on the radical scavenging activity of N-alkyl moieties, but also on the associated crosslinking that takes place under processing conditions. Some exploratory results from a solid-state ^{13}CNMR analysis provide support to a radical mechanism, involving coupling between benzyl-like pyrrolyl species.

1. Introduction

One of the most important challenges in polyolefin research today is to modify their inherent non-polar nature by the controlled insertion of chemical groups, capable of conferring special properties, mainly the ability to interact with other materials or media and reactivity for subsequent attachment of specific functionalities, in order to achieve high performance materials.

In this context, polyolefin functionalization has arisen as a way to circumvent drawbacks associated to the stabilization by using external additives [1,2]. On the one hand, stabilizers do not improve the intrinsic thermo-oxidative stability of polyolefins since they just delay degradation. Actually, their mechanisms of action are based on the deactivation of radicals, mainly generated from the homolytic scission of hydroperoxides during the earliest stage of the degradation [3]. Therefore, after exhaustion, polyolefin chain degradation proceeds. On the other hand, stabilizers are not compatible enough with polyolefins to prevent them from migration towards the surface and loss, thereby, leading to a decrease in long-term stability.

Simple insertion of stabilizing functions into polyolefin chains can solve the migration problem [4–8], however, improving inherent stability is not an easy task, because it requires to modify the material's thermal response to heating, in terms of chain mobility and diffusivity of oxygen. Nevertheless, Chung's results have shown that functionalization of polyolefins is, indeed, a promising methodology to meet this goal. In particular, they have reported the functionalization of PP with a hindered phenol, which undergoes dimerization through radical activation and, therefore, crosslinking with the desirable stabilization effect [8–12]. Moreover, such functionalized PP has been found to perform better against thermo-oxidation than classical stabilizers, when blended with the PP homopolymer, because of its high compatibility [9–12].

Among the different strategies followed to functionalize polyolefins, direct copolymerization of olefins with polar vinyl monomers is the shortest and simplest way to suitably tune the microstructure in composition, as well as chain stereo-microstructure in the case of proquiral monomers and molecular weight, according to the final application [13,14]. Unfortunately, this route poses some major problems derived from the incompatibility between transition metal catalysts used

* Correspondence to: Instituto de Ciencia y Tecnología de Polímeros (ICTP), Consejo Superior de Investigaciones Científicas (CSIC), 28006 Madrid, Spain.
E-mail address: elvira@ictp.csic.es (J.M. Gómez-Elvira).
[1] orcid.org/0000–0003-2488–5635
[2] orcid.org/0000–0002-2366–2117
[3] orcid.org/0000–0003-0535–1048

https://doi.org/10.1016/j.mtcomm.2022.103469
Received 2 December 2021; Received in revised form 28 February 2022; Accepted 29 March 2022
Available online 2 April 2022

and monomers bearing electron pairs available for coordination, leading to poisoning of active sites. This makes it necessary to resort to protection of polar groups, including the use of intermediate catalyst-compatible functions from which the pursued functionality can be eventually obtained, which ultimately makes this methodology expensive and time-consuming.

Notwithstanding the above constraints, polyolefins functionalization would be an excellent methodology to produce highly effective stabilization, if a one-step synthesis of the modified polyolefin could be developed. This requirement, together with a low cost, are mandatory for an eventual industrial scale-up. The present study aims at making progress towards these objectives.

An ideal scenario would be the direct synthesis of the reactive polyolefin by copolymerization and its subsequent transformation into a more stable material, by taking advantage of conditions under which the material is finally processed. In the search for a suitable functionality that meets these requirements, N-alkyl pyrrole compounds have been identified as species able to react, under the catalytic action of decomposing PP hydroperoxides, to form dimers by radical coupling [15]. Such peculiarity would allow not only to trap the radical activity in the early stages of the oxidation, but also to create link points between PP chains that would provide mechanical and thermal stability.

This study outlines the synthetic aspects and the stability performance of poly(propylene-*co*-1-(undec-10-ene-1-yl)-*1 H*-pyrrole) copolymers, as a model case to test the feasibility of the above commented N-alkylpyrrole chemistry into a polyolefin matrix. The final aim is to assess the benefits these materials may offer, not only from the point of view of the stability, but from the self-healing ability under high temperature conditions. Special attention has been paid to the identification of residual species (i.e. isomers), contained in the synthesized pyrrole comonomer, to thoroughly account for the oxidation evolution of the materials at high temperature and in air atmosphere.

2. Experimental part

2.1. Materials

2.1.1. Synthesis of monomers

The synthesis of 1-(undec-10-ene-1-yl)-*1 H*-pyrrole [**PyI**], as well as that one of a ternary mixture of 1-(undec-10-ene-1-yl)-*1 H*-pyrrole [**PyI**], 2-(undec-10-en-1-yl)-*1 H*-pyrrole [**PyII**] and 3-(undec-10-en-1-yl)-*1 H*-pyrrole [**PyIII**] is detailed in the supplementary material.

2.2. Synthesis of the polypropylene and copolymers

The homo and copolymerization reactions were performed under inert conditions and after careful purification of the reagents. Toluene (Merck) was dried by refluxing over metallic sodium and further distillation under nitrogen. Nitrogen (Praxair 3X) and propylene (Praxair 2.5) were purified by flowing through oxygen-trap columns and molecular sieves before using. The metallocene catalyst *rac*-dimethylsilylbis(1-indenyl) zirconium dichloride ($Me_2Si(C_9H_6)_2ZrCl_2$) was supplied by Strem, and the co-catalyst MMAO was supplied by Sigma-Aldrich, as a solution in toluene (MMAO-12, 7 wt% in Al).

Polypropene homopolymers and poly(propene-*co*-1-(undec-10-ene-1-yl)-*1 H*-pyrrole) copolymers were prepared in a 100 mL glass vessel at a polymerization temperature (T_{pol}) of 25 ºC, in 50 mL of toluene and with an initial propene pressure of 1.5 bar. The [Al]/[Zr] molar ratio used was 3077.

In the case of co-polymerizations, prior to the addition of the activated metallocene precursor (1.3 μmol), the solution of propylene, PyI and MMAO (2.5 mL/0.004 moles), was allowed to stir during 45 min to block the functional comonomer by interaction with the co-catalyst. The reactions were finished after a 10–20% propene consumption by adding 5 mL of ethanol. Subsequently, samples were precipitated with a mixture of ethanol (Aroca, 96%) and HCl (VWR, 37%) (30:1). The so-precipitated polymers were washed in ethanol overnight under lively agitation, filtered, washed again with fresh ethanol and, finally, dried under vacuum at room temperature.

Henceforth, samples shall be designated as PP for the polypropylene homopolymer and PPy for the copolymers, followed by the pyrrole content in mole percent. Data of polymerization runs are shown in Table 1.

2.3. Processing of samples

Homo and copolymers were processed as films in a Collin press between hot plates, using a pressure of 2.5 MPa, for 2 min and at a temperature of 30 °C above their melting points. The films were subsequently cooled down to room temperature, by rapid cooling between plates refrigerated with water.

2.4. Thermal treatment of samples

The PPy-2.6 sample was heated by using a tubular furnace at 10ºC/min up to 200ºC, in a 20 L/h air flow, and then exposed at that these conditions for 0, 30, 120 and 240 min. Finally, the sample was chilled by switching off the power supply. Final specimens are referred as PPy-2.6, followed by the exposure time in minutes.

2.5. Microanalysis

The elemental analysis of the insoluble copolymer was performed in a micro-analyser *LECO CHNS-932*, at a combustion temperature of 990 ºC and using He as carrier gas. Average values of C, H and N weight percentages were calculated from three measurements per sample.

2.6. Nuclear magnetic resonance

The ^{1}H NMR spectrum of both the PyI comonomer and the mixture of PyI/PyII/PyIII comonomers were obtained with a *Bruker Avance III HD-400*, in $CDCl_3$ solution, at room temperature. ^{1}H and ^{13}C NMR analysis of the most soluble copolymer were carried out in 1,1,2,2-tetrachloroethane-d_2 (TCE-d_2) solutions (70 mg•0.7 mL^{-1}), by using a *Bruker Avance III HD-400* at 80 ºC. In the case of the PP homopolymer and the copolymer with the lowest solubility, PPy-0.6, a *JEOL JNM-ECZ400R* equipment at 100 ºC was used.

^{1}H NMR spectra were recorded accumulating 64 scans. As for ^{13}C NMR, spectra were recorded with broad band proton decoupling, using a 24038 Hz spectral window, an acquisition time of 1 s, a relaxation delay of 5 s, a pulse angle of 45º (5 μs) and a minimum of 8000 scans. Chemical shifts for ^{1}H and ^{13}C NMR signals were referred to those ones of the 1,1,2,2-tetrachloroethane-d_2 at 6.00 and 74.00 ppm, respectively.

The 2D ^{1}H–^{13}C DEPT-HSQC spectrum of the **PyI**/**PyII**/**PyIII** mixture was performed using a 90º pulse (14 and 10 μs for ^{1}H and ^{13}C, respectively), 6.39 MHz spectral width in the ^{1}H dimension and 16.59 MHz in the ^{13}C dimension, 0.2 s acquisition time and 2 s relaxation delay.

The partly soluble processed copolymer PPy-2.6 was characterized by means of solid state CP/MAS ^{13}CNMR analysis, in a *Bruker Avance Neo 400 MHz*, with zirconia rotors (⌀ext. 4 mm) at 9000 Hz, 3 s of pulse delay and 2000 scans. A 90º pulse, 4 s for the ^{1}H nucleus was used with a contact time of 1 ms and dipolar decoupling for 0.05 ms.

2.7. Infrared spectroscopy

FTIR spectra were recorded by performing 4 scans in a *Perkin Elmer Spectrum Two* spectrometer, in the 4000–450 cm^{-1} range and with a resolution of 4 cm^{-1}. In the case of the PyI comonomer, as well as of the PyI/PyII/PyIII mixture, it was recorded from a thin liquid layer applied on a PP film. The corresponding spectra were obtained by subtracting the PP substrate spectrum from the raw spectra. For PP and copolymers, spectra were obtained from films processed under the conditions

Table 1
Data of polymerization runs.

Sample	[Py]/[Propylene] Feeding ratio	Py content (mol%)	Time (min)	Weight (g)	Mn ($g \cdot mol^{-1}$)	Global activity ($Kg \cdot mol_{[Zr]}^{-1} \cdot h^{-1}$)
PP	0	0	10	1.37	42000	6489
PPy-0.6	0.013	0.6	33	0.87	47400	1239
PPy-1.2	0.033	1.2	208	0.99	38300	206
PPy-1.5	0.038	1.5	201	1.12	34300	241
PPy-2.4	0.067	2.4	145	0.93	38700	303
PPy-2.6	0.066	2.6	169	1.50	34400	419
PPy-5.3	0.13	5.3[a]	207	0.34	–	77

a) Calculated from microanalysis

described above. The spectra of polymer samples were baseline corrected and normalized to the intensity of the 2722 cm^{-1} peak.

2.8. Differential scanning calorimetry

DSC runs were performed in a *TA Q100 Instrument* calorimeter connected to a cooling system and calibrated with Indium and Zinc. The films of the samples were heated from − 60 ºC to either 160 °C for the copolymers or 180 °C for the PP sample, at a heating rate of 10 °C·min^{-1}. They were subsequently cooled down to − 60 °C, also at 10 ºC·min^{-1}, and finally heated again up to 160 or 180 °C. The values of the melting temperature (T_m) and crystallinity (F_c) were taken from the maximum and the enthalpy of fusion of the 2nd run's endotherm peak, respectively. For the estimation of the crystallinity, a value of 162 J•g^{-1} was taken as the melting enthalpy of a 100% crystalline iPP [16].

2.9. Thermo-gravimetric analysis

TGA runs were carried out in a *Thermal Analysis TGA-Q 500* device. The samples used were 4 mm discs, cut from the films with a calibrated die. Heating ramps from 50 ºC up to 750 ºC at 2, 5, 10 and 20 ºC•min^{-1} were used, under a 90 mL•min^{-1} flow of either nitrogen or air.

2.10. Determination of the gel fraction

The evolution of the gel fraction for the copolymer PPy-2.6, molten in air flow (20 L·min^{-1}) up to 200ºC (10ºC·min^{-1}) and subsequently heated at these conditions for increasing exposure times (0, 30, 120 and 240 min), was calculated by using xylene as extracting solvent, at 90 °C and during 2 h. The selected temperature was chosen to avoid the evolution of the cross-linking degree during the experiment.

3. Results and discussion

3.1. Copolymerization kinetics

Metallocene catalysts are very sensitive to the presence of comonomers bearing heteroatoms, with which the metal atom can be coordinated [13,14,17,18]. That is the reason why an olefin bearing a pyrrolyl moiety (Py) was expected to slow down the propylene polymerization kinetics. The comparison of the propylene consumption rates, shown in Fig. 1, makes evident that a negative kinetic effect of the Py comonomer takes place. The evolution of the maximum reaction rate fits an exponential decay (Fig. 2) and leaves no doubt that the concentration of active centres strongly decreases with the [Py]/[Propylene] ratio. This marked blocking character is the only inhibiting action expected, since the long spacer between the pyrrole moiety and the olefin allows to assume that the electronic characteristics of the double bond remain untouched. Data concerning the different runs performed are collected in Table 1, where it is apparent how the global activity follows a decreasing trend, when the Py content increases. Likewise, it was also expected that the termination rate of the polymerization would be affected. The average polymerization degree (DP) obtained by means of ^1H NMR allows the estimate of the apparent termination rate, if it is assumed that the DP value results from the ratio between propagation (R_p) and termination (R_t) rates [19]. The value of the reaction rate at the maximum (Fig. 1) has been taken as a measure of R_p, since the subsequent decrease is the effect of multiple factors, one of which is the trapping of active sites into the precipitated polymer, which hinders the access of the comonomers.

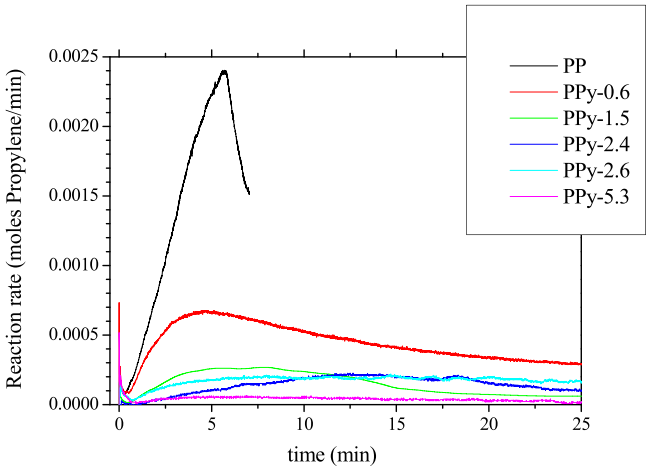

Fig. 1. Evolution of propylene consumption with time in the synthesis of PP and Py materials. A color code is inserted into the figure.

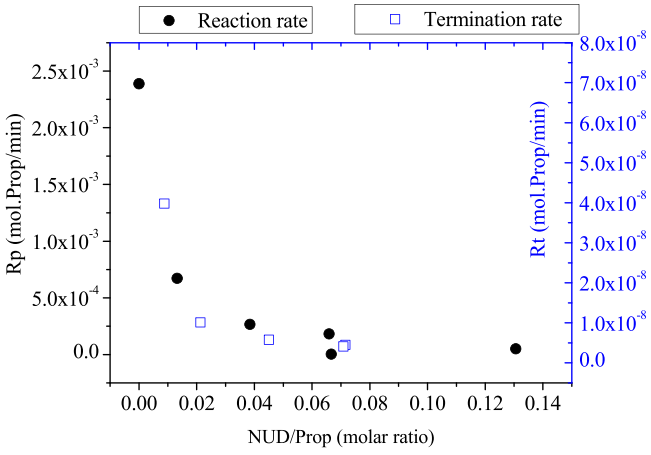

Fig. 2. Evolution of the termination and maximum propagation rates with the Py/Propylene ratio in the feeding.

The evolution of R_t with the Py/Propylene in the feeding is shown also in Fig. 2 and evidences that the termination kinetics is one order of magnitude lower than that one of the homo-polymerization, at very low Py contents. Accordingly, similar decreasing trends for the propagation and termination rates, with the Py content, confirm the driving effect of the interaction between the Py molecule and the active site.

3.2. Microstructure of copolymers

3.2.1. Composition and molecular weight (NMR & FTIR)

The composition range covered in this studied is restricted to low Py contents (ca. up to 5 mol%) due to the fact that copolymers, although still elastic and mouldable, become quite insoluble beyond 3 mol% and characterization in solution becomes impossible. In fact, the composition of PPy-5.3 was obtained by microanalysis. The reported radical chemistry associated to N-alkyl pyrroles, in the presence of hydroperoxides [20], is thought to lie behind a crosslinking process when heating the copolymers during either processing or dissolution. Such a process must occur in all copolymers, but it must be critical at a certain conversion level, when the percentage of bound pyrroles is sufficient to prevent complete solubilisation of the copolymer.

In contrast to that, samples below 3 mol% are completely soluble under usual NMR characterization conditions for polyolefins. Their ^{1}HNMR spectra exhibit signals corresponding to copolymers that contain Py units, as it is displayed in Fig. 3 for the case of sample PPy-2.6 as an example. This figure shows the different nuclei that have been used to calculate the comonomer content. In particular, the relationship between $1B_9$ protons and main-chain methyne protons (brB_1) was chosen to know the copolymers composition. Such nuclei have been identified according to the nomenclature shown in Chart 1 [21]. Fig. 4 shows how, in this short conversion range, the correlation between Py contents in the copolymers and in the polymerization feeding is quite linear. A more detailed analysis of the ^{1}HNMR spectrum of copolymers allows to remark the presence of some residual signals, ascribed to the presence of a quite small proportion (about 6 mol.% of the total Py groups) of the two possible isomers of the Py comonomer, i.e. the 2- and 3-alkyl substituted species (species II and III in Chart 1). Such isomers are detected by distinctive N-H protons at 7.87 and 7.94 ppm, together with their respective triplets at 2.62 and 2.52 ppm pertaining to $1B_9$ methylenes groups. These ^{1}HNMR signals are consistent with the FTIR peaks at 3405 and 3487 cm^{-1} (see FTIR spectra of copolymers in Fig. S2) that clearly show the existence of N-H bonds. The identification of the Py isomers is worth considering, in view of their response against oxidation.

The analysis of the distribution in composition is shown in Table 2 and it has been performed by means of ^{13}CNMR, from the relative intensity of the signals corresponding to the nuclei $1B_9$, $\alpha\alpha B_1B_9$ and brB_1 (Chart 1). Such signals are shown in Fig. 5 that displays the complete assignment of the carbon nuclei, for the case of the PPy-2.6 copolymer. The resulting microstructure corresponds to random copolymers containing isolated comonomer units only, and exhibiting decreasingly propylene average lengths. This fact is the origin of the drop in both crystallinity and melting temperature in PP copolymers and, accordingly, one would expect that composition had a detrimental impact in those applications where stability against oxidation and mechanical strength were required, if there were no other effects than the simple comonomer insertion.

With respect to chain size, the thermal reactivity of the copolymers

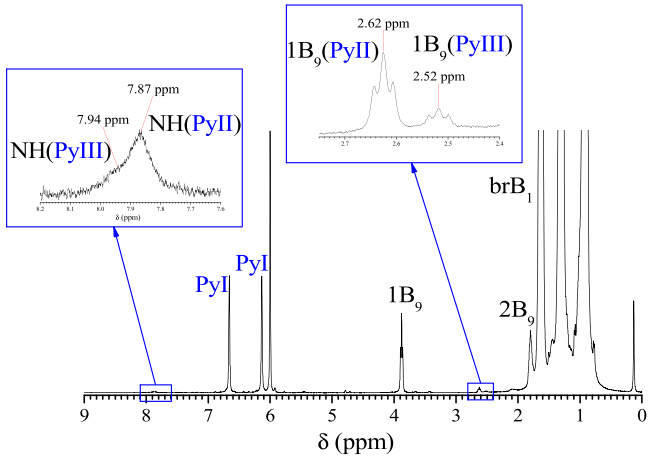

Fig. 3. ^{1}HNMR spectrum of PPy-2.6 in $C_2D_2Cl_4$ at 80ºC.

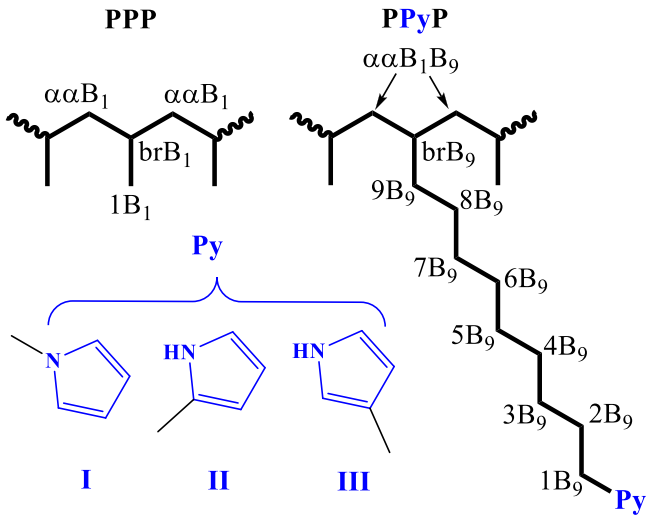

Chart 1. Nomenclature of carbon nuclei in PPP and PPyP triads.

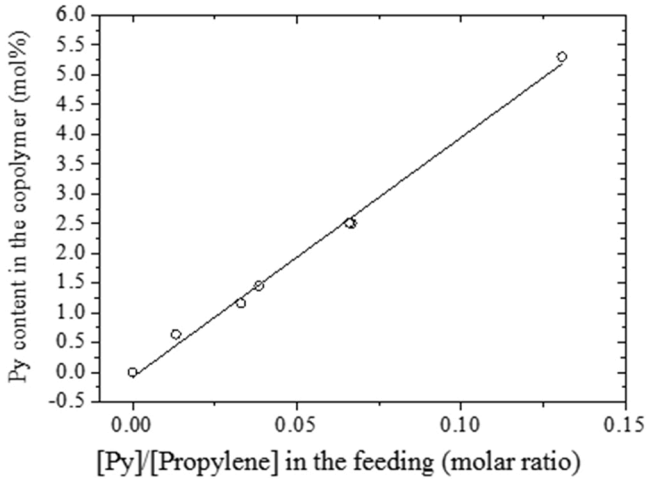

Fig. 4. Correlation between the Py content in the copolymers and in the copolymerization feeding.

Table 2
Compositional distribution at the triad level and propylene average length.

Sample	PPP (mol%)	PPX (mol %)	XPX (mol%)	PXP (mol %)	XXP (mol%)	XXX (mol%)	n_p[a]
PPy-0.6	98.29	1.15	0	0.56	0	0	174
PPy-1.2	95.53	2.77	0	1.70	0	0	71
PPy-1.5	95.52	2.65	0	1.84	0	0	74
PPy-2.4	92.67	4.78	0	2.54	0	0	41
PPy-2.6	92.48	4.79	0	2.73	0	0	41

a) Propylene average length calculated from the expression: $n_p = ([PPP]+[PPX]+[XPX])/([XPX]+½\cdot[PPX])$

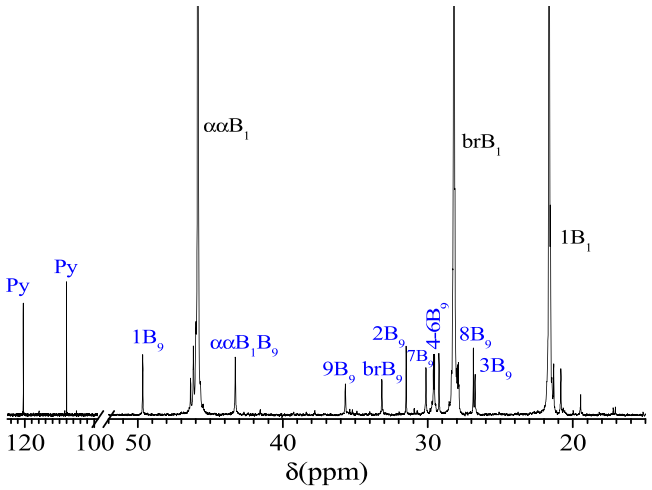

Fig. 5. ^{13}CNMR of PPy-2.6 in $C_2D_2Cl_4$ at 80ºC.

prevents them from measuring the average molecular weight (M_n) by means of GPC, under usual conditions for polyolefins, i.e. at 140ºC. In addition, the accuracy of GPC for polar polyolefins has been called into question [22–24]. Consequently, ^{1}H NMR has been used to estimate the molar mass of the copolymers, assuming that the main termination mechanisms of chain growing are those producing a chain-end olefin [25,26]. Other termination mechanisms leading to alkyl chain end-groups, such as chain transfer to the co-catalyst (MMAO), are also assumed to be residual under the reaction conditions used in the study.

The inspection of the ^{1}H NMR olefinic window of the samples (Fig. S5) reveals that vinylidene chain-ends (V_d), arising from terminal 1,2-propylene units, and vinylene chain-ends (V_y), coming from both terminal 2,1-inserted propylene and Py units, are produced and may be used to assess the M_n values on the basis of the above considerations. The results in Table 1 show that the PPy copolymer with lowest comonomer content (PPy-0.6) retains a high M_n value, which decreases weakly for higher contents to a roughly constant value. Such trend suggests that pyrrole groups do interact with catalyst sites and make chain termination processes more difficult to occur. Actually, the insertion of other nitrogen containing comonomers has been reported in literature [27] to raise the molecular weight of polypropylene-based copolymers. Such effect is the result of the above indicated hindered termination mechanisms, and is bound to the partially blocking interaction of the polar comonomer with the catalyst.

3.2.2. Configuration (^{13}C NMR)

The analysis of tactic distributions of propylene sequences, collected in Table 3, reveals a slight increase in the content of isotactic pentads, when PP and PPy-0.6 samples are compared. Although this difference might evidence an improved isoselectivity of catalyst centres, as it has already been described for other polar comonomers, like amino-olefins [27], such behaviour does not seem to be confirmed when considering higher pyrrole contents. Consequently, the only effect of the interaction of pyrrole groups with active sites appears to be a reduction of the catalyst activity, without any change in the insertion stereochemistry.

3.3. Evolution of copolymer morphology with heat treatment

The melting and crystallization curves of pristine copolymers are displayed in Figs. S6 and S7, and their corresponding parameters collected in table S1 (supplementary materials). The decreasing evolution of both the crystalline content and the distinctive temperatures, with the Py content, confirm the expected effect of shortening propylene sequences on thermal properties. Concurrently, Tg decreases 26ºC from PP up to PPy-5.3 as a result of an increasingly mobile amorphous phase, as the pyrrole content rises.

The most interesting feature of these materials is the generation of an increasing degree of crosslinking over time in heat treatment under air. This was tested in the PPy-2.6 sample when heated in air flow at 10ºC/min, up to 200ºC, then exposed at that temperature for different times. The decrease of the soluble fraction in xylene at 90ºC, displayed in Fig. 6, is definitely attributed to inter-chain linkage with heating time and is reasonably associated to pyrrole reactivity. As a matter of fact, N-alkyl pyrroles are able to yield benzyl-like radicals, under the action of decomposing peroxides with temperature, which eventually generate dimers by coupling [20]. A similar scenario must exist in the copolymer matrix, since either hydroperoxides in PP chains or oxygen, or both, may act as radical initiators and then cause di-pyrrole connections, as shown in Scheme 1.

After erasing the thermal history of the heat-treated PPy-2.6 samples, by performing a first melting cycle at 10ºC/min up to 160ºC, the crystallization and the subsequent second melting processes were tracked at the same heating speed. It is clear from table S1 that the crystallinity of the PPy-2.6, measured from both the crystallization and the 2nd melting runs, hardly changes by heating in an airflow up to 200ºC, followed by

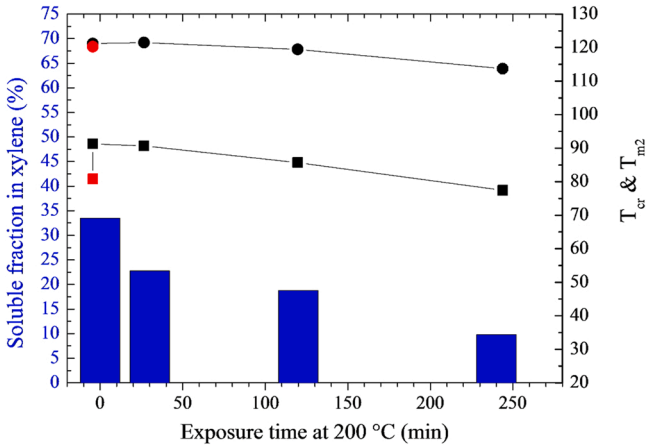

Fig. 6. Evolution of soluble fraction and crystallization (T_{cr} ■) and melting temperatures (T_{m2} ●) in PPy-2.6 with exposure time at 200ºC in air. Red points correspond to T_{cr} and T_{m2} values for the film processed at 160ºC. (For interpretation of the references to colour in this figure legend, the reader is referred to the web version of this article.)

Table 3
Tactic distribution of propylene sequences at the pentad level.

Muestra	mmmm	mmmr	rmmr	mmrr	mmrm + rmrr	mrmr	rrrr	mrrr	mrrm	Regio defects	n_i[a]
PP	89.6	3.1	1.1	3.6	1.4	0	0	0	1.1	0.1	39
PPy-0.6	92.4	3.0	0.1	2.4	0.6	0	0	0	1.0	0.5	48
PPy-1.2	89.1	3.7	0.7	3.2	1.3	0	0	0	1.3	0.7	65
PPy-1.5	90.0	3.5	0.5	3.1	1.2	0	0	0	1.1	0.6	43
PPy-2.4	89.1	3.2	0.5	3.2	1.7	0	0	0	1.0	1.3	46
PPy-2.6	91.9	2.9	0.3	2.6	1.0	0	0	0	0.7	0.6	40

a) Isotactic average length: $n_i = ([mm]+[mr])/(½\cdot[mr])$

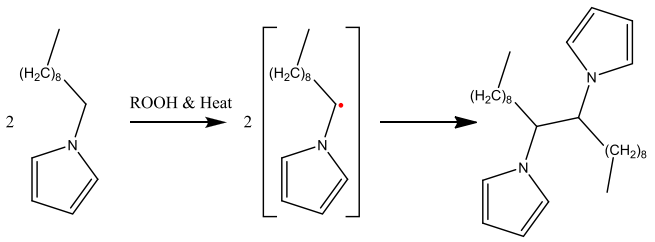

Scheme 1. Generation and combination of pyrrolyl-methylen radicals.

30 min exposure time. However, longer treatments cause the crystallization ability to decrease significantly, as it is also reflected by means of the crystallization and melting enthalpies. Concomitantly, crystallization (T_{cr}) and melting temperatures (T_{m2}) remain almost unchanged during the first 30 min of heating, but both shift downwards for longer times (Fig. 6). Therefore, it is clear that crosslinking has a gradual effect on the crystalline content of PPy-2.6. However, despite the T_{cr} decrease, there is a striking initial increase (ca. 10 °C) by comparing the pristine sample with the one that has been simply melted at 200 °C ((PPy-2.6–0, Fig. 6). This fact might reveal how copolymer chains in the molten state are compelled to crystallize at significantly higher temperatures, due to mobility restrictions imposed by the crosslinking or because of the nucleating effect of tiny amounts of crosslinked copolymer. Additionally, it could be the effect of proper chain relaxation undergone by the copolymer, when processed at 200ºC. The fact that the subsequent melting temperature (T_{m2}) remains the same as that of PPy-2.6 (around 120ºC, Fig. 6) shows that the quality of crystals was not altered by the 200ºC treatment, but that chains were forced to be ordered earlier.

Finally, T_g correlates directly with the appearance of mobility constraints in the amorphous phase when heating the copolymer, as it is reflected in table S1 by its upward shifting, which is also a conclusive evidence of the crosslinking progress.

3.4. Thermal stability of copolymers

3.4.1. Stability in air

The comparison of the TGA curves (Fig. S8 to S11 in supplementary material) shows that there is a net shift of the temperature at which the weight loss starts (T_i), for a Py content as low as 0.6 mol%. Secondly, it is also evident that T_i keeps on shifting upwards as far as the Py content increases, although the stabilization does not go further from sample PPy-2.6 onwards, when the degradation is clearly a multistep process (see DTGA curves in the supplementary material - Figs. S8 to S11).

The improved endurance against oxidation of PPy copolymers is quantified in Fig. 7. The upward progression of T_i meets a maximum at 2.6 mol% of Py comonomer, which corresponds to an increase of about 80ºC at 2 ºC/min. This change is ascribed to the crosslinking process caused by N-alkyl pyrrole moieties in the presence of oxygen, which makes the material not only to resist higher temperatures but also to suppress the previous oxygen uptake to volatiles release, i.e. the characteristic hydro-peroxide build-up of PP thermo-oxidation. It is clear then that crosslinking is directly related to the observed improvement in stability, as this process consumes either hydroperoxides or oxygen, or both, thus preventing the material from oxidation but, in addition, it also produces chain mobility restrictions that likely lead to oxygen diffusion limitations. It is also evident that crosslinking takes place progressively during the TGA heating run, making it important for the evaluation of resistance against oxidation at constant temperatures below the melting point, when the crosslinking kinetics slow down. Anyway, the fact remains that the copolymers become much more stable simply by processing and even more so at high operating temperatures, because of the radical scavenging activity of N-alkylpyrroles and their subsequent coupling.

3.5. Stability in N_2

In a similar way, the insertion of Py co-units in PP chains delays the release of volatiles in inert atmosphere. The evidence of this is shown in Figs. S12-S15 that collect the characteristic single-step weight loss processes of polyolefin pyrolysis and their corresponding DGTA curves.

In this case, the thermal performance achieved is lesser than that observed in air, since it is hardly 10ºC for PPy-2.6, as it is shown in Fig. 8. Nevertheless, what it seems to agree with thermo-oxidation is the fact that the T_i increment reaches its maximum well before the highest Py content studied (PPy-5.3). Although this stabilization effect is linked to the Py units, the mechanism underlying would be different to the one suggested in air. It has been reported that pyrolysis of N-alkyl pyrrole species (c.a. 460–570 ºC) [28–30] involves isomerization to the 2 and 3-alkyl substituted pyrroles and subsequent minor decomposition of the C-substituted pyrroles through radical species. Such a scenario into the PP matrix might eventually lead to chain interconnection between pyrrole groups, rather than to chain scission, as it usually occurs in normal PP pyrolysis, and could justify the increase of T_i in the copolymers.

3.6. Mechanism of stabilization in air

Previous solution NMR analysis could not cover samples after processing and after undergoing high temperature treatments, because

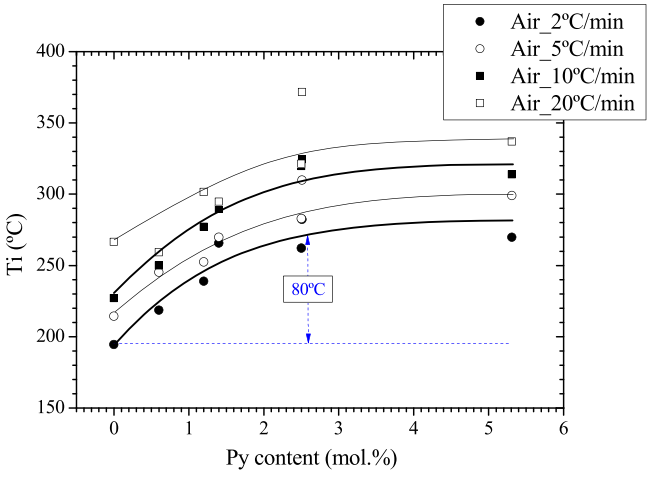

Fig. 7. Evolution of the weight loss onset temperature (Ti) with the Py content in air, at different heating rates.

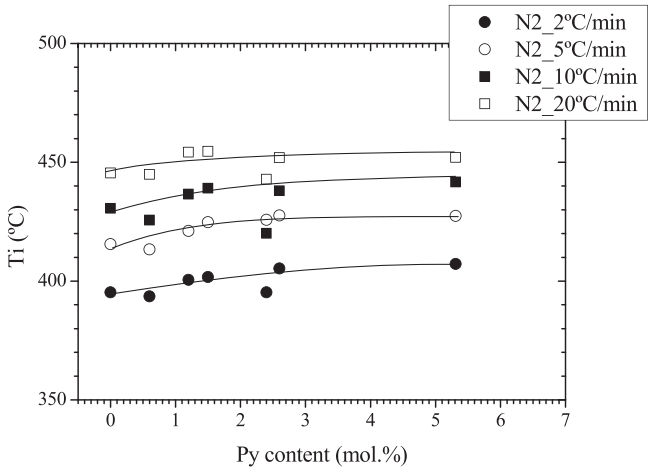

Fig. 8. Evolution of the weight loss onset temperature (Ti) with the Py content in N_2, at different heating rates.

samples became partly insoluble. Therefore, the analysis of the microstructure at the molecular level has been carried out by means of solid ^{13}C NMR and FTIR to identify, at least qualitatively, the chemistry beneath both the crosslinking phenomenon and the eventual oxidation processes.

3.6.1. FTIR

The comparison of the FTIR spectra of the processed samples allows tracking the Py content in the PPy series, mainly by means of the 720 cm^{-1} peak that is ascribed to the deformation mode of pyrrole C-H bonds (see Fig. S2 in supplementary materials). Additionally, the analysis of low intensity peaks, corresponding to carbonyls and hydroperoxides windows, in Fig. 9 gives some interesting details. Concurrently with the above mentioned presence of the 3405 cm^{-1} and 3487 cm^{-1} peaks, two other signals at 1705 cm^{-1} and 1665 cm^{-1} show up. These two peaks correspond to lactams caused by the oxidation of pyrrole groups, whose origin seems to be mostly in the oxidation of N-H pyrrole groups (isomers PyII and PyIII in Chart 1). This is what can be inferred from the evolution of corresponding FTIR peaks, when the PPy-2.6 and PPy-5.3 copolymers are heated at 200ºC in air. Fig. 10 shows how the increase of lactams with heating time (1665 and 1706 cm^{-1}) leads to a substantial vanishing of pyrrole NH vibration modes (3405 and 3487 cm^{-1}), when both samples are heated for quite some time (240 min). This is another oxygen-consuming mechanism that might contribute to the stabilization of the material.

3.6.2. ^{13}C NMR

In an attempt to confirm the aforementioned stabilization mechanism, the evolution of the ^{13}C NMR spectrum of sample PPy-2.6, thermally treated in an air flow at 200ºC, has been tracked over time. The ^{13}C NMR spectra series obtained is shown in Fig. 11, which collects only the window corresponding to pyrrole carbons, given that no changes were found in the aliphatic carbon region (10–50 ppm).

Even though the low intensity of the signals into the 100–140 ppm range precludes an accurate quantitative analysis, the estimation of their relative intensities allows withdrawing some conclusions, which are compatible with the mechanism proposed in Scheme 1. Firstly, together with peaks at 109 and 120 ppm in the pristine PPy-2.6 powder, ascribed to carbons of N-alkyl pyrrole rings (PyI), three other ones exist placed at 111, 116 and 134 ppm, whose intensity level is much higher than it would be expected for chain end double bonds detected in ^{1}H NMR analysis. In particular, vinylidene and vinyl groups. Accordingly, these signals are tentatively attributed to pyrrole carbons of comonomer isomers (PyII and PyIII in Chart 1). As a matter of fact, these species have been found to exhibit ^{13}C signals close to these specific shifts in solution

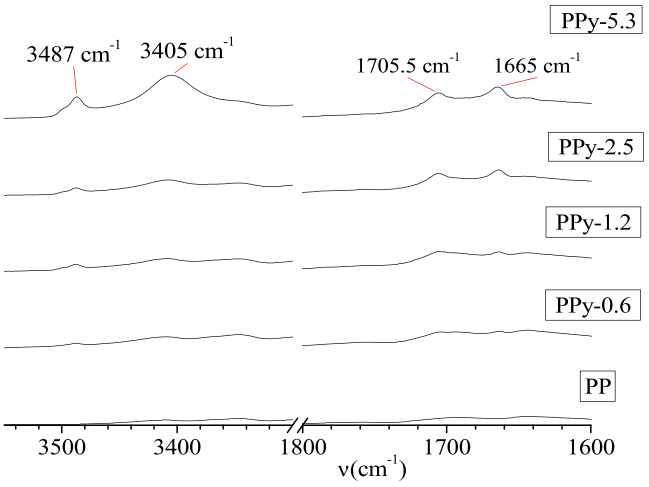

Fig. 9. Normalized FTIR spectra of processed samples in the specified windows.

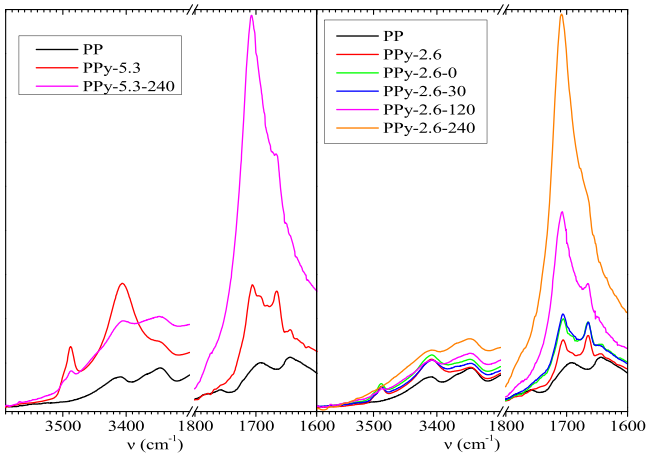

Fig. 10. Evolution of FTIR spectra in the specified windows of PPy-2.6 (right) and PPy-5.3 (left) films over time, at 200ºC in air. Processed samples of PP, PPy-2.6 and PPy-5.3 are displayed for comparison. A color code is inserted into the figure.

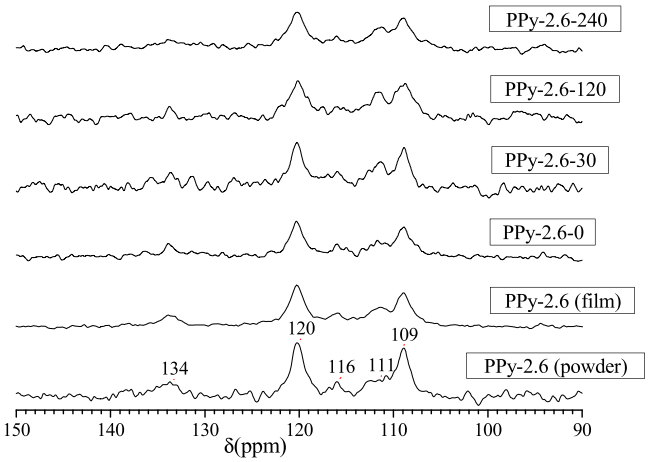

Fig. 11. Evolution of ^{13}C NMR pyrrole window of PPy-2.6 with hot-press processing and further treatments at 200ºC in air flow.

(see ^{13}CNMR peaks for PyI/PyII/PyIII in experimental section and spectrum in Fig. S4 in $C_2D_2Cl_4$ at 80ºC). Furthermore, the assignment of these signals to PyII and PyIII isomers is consistent with the solubility of the virgin PPy-2.6.

Secondly, the hot-press processing at 30ºC above the melting point causes the partial vanishing of the 109 ppm peak. In the absence of other signals, this fact may be associated with the crosslinking occurring between N-alkyl pyrrole unis (Scheme 1), since such simple thermal treatment yields the material partially insoluble. In a supplementary way, chemical shifts predicted for the 109 ppm pyrroles carbons are slightly low field shifted, when crosslinked as shown in Scheme 1. The relative increase of the 111 ppm centred peak at ever-increasing heating times at 200ºC (Fig. 11), provides some support to this hypothesis.

Finally, while the evolution of the 116 ppm peak with time at 200ºC is difficult to assess, the 134 ppm one seems to disappear. The former is actually distinctive of PyII and PyIII species but, both the low intensity and the marked overlapping, make its evolution unreliable. On the contrary, the 134 ppm peak unequivocally tends to decrease. Such peak is assigned to PyII, that is, to one of the isomers involved in the oxidation process at long heating times, as it was observed by the decline of the NH stretching mode at 3405 cm^{-1} for PPy-2.6 and PPy-5.3, after undergoing a 240 min long treatment at 200ºC (Fig. 10). Unfortunately, the intensity variation level of signals, due to Py oxidation, is small and a definitive

^{13}C NMR confirmation of this hypothesis, by detecting carbonyls associated to lactams (170–180 ppm) [31], was not possible. On account of these facts, the crosslinking mechanism depicted in Scheme 1 is therefore the most plausible one. Other involving interring couplings like formation of 2 and 3-pyrrolyl-methylene-pyrroles [20] cannot be excluded, but are less likely because of the lack of associated ^{13}C NMR signals.

4. Conclusions

The synthesis of functionalized PP containing pyrrole groups is feasible by direct metallocene copolymerization of the propylene with the 1-(undec-10-ene-1-yl)-*1 H*-pyrrole. Although the accessible conversion range for the preparation of soluble materials is limited to pyrrole contents under 3 mol%, the materials exhibit high enough molecular weights, i.e. comparable to that one of the reference PP, and improved isotacticity in the propylene sequences. These two facts are thought to be related with the specific interaction of pyrrole groups with active sites, which, on the one hand, slows down both chain propagation and chain termination events and, on the other, enhances spatial requirements for monomer coordination.

The soluble copolymers undergo some crosslinking under processing conditions, while retaining both apparent processing ability and flexibility. Such crosslinking can be increased after processing by further heat treatment, and this process is shown to be the underlying reason for the high thermal stability of these materials. The qualitative analysis of the evolution of pyrrole units during heat treatment, by means of solid-state ^{13}CNMR analysis, supports the hypothesis of a radical coupling mechanism between N-alkylpyrrole pendant groups, which would be activated either by oxygen or PP hydroperxides or both of them.

The improvement in thermal stability against oxidation is significant for a pyrrole content as low as 0.6 mol.% and it increases for higher contents, reaching degradation temperatures about 80ºC higher than the virgin PP, for the copolymer with 2.6 mol.% of pyrrole units.

From the point of view of practical applicability, it is clear that a balance between productivity, stability improvement and crosslinking ability must be stablished to scale-up the production of these copolymers. On account of the large thermo-oxidative stability found for pyrrole contents as low as 0.6 mo%, modification levels up to 1 mol% are the most reasonable option to get high thermal stability PP thermoplastics. Moreover, the production of low-modified PP to be used not only as high-performance materials, but as special additives, might be a realistic alternative. In fact, this option would be the most plausible to combine a significant stability improvement of PP grades with a more cost-effective production. At this stage of the research, it is clear that the detailed synthesis of these copolymers do not fit industrial requirements for large-scale production and further work should be carried out to optimize reaction conditions.

Funding sources

Consejo Superior de Investigaciones Científicas (CSIC: Project PIE202060E215).

CRediT authorship contribution statement

All authors have given approval to the final version of the manuscript.

Declaration of Competing Interest

The authors declare that they have no known competing financial interests or personal relationships that could have appeared to influence the work reported in this paper.

Acknowledgment

The financial support from project Polymeric Nanodielectrics, Proyecto Intramural Especial, PIE202060E215 (CSIC, Spain) is greatly acknowledged.

Supplementary materials

Synthesis of [PyI]: 1-(undec-10-ene-1-yl)-*1 H*-pyrrole; Synthesis of a ternary mixture of [PyI]: 1-(undec-10-ene-1-yl)-*1 H*-pyrrole, [PyII]: 2-(undec-10-en-1-yl)-*1 H*-pyrrole and [PyIII]: 3-(undec-10-en-1-yl)-*1 H*-pyrrole; (Table S1) DSC values of glass transition, melting and crystallization temperatures and crystallinity; (Figs. S1-S5) ^{1}HNMR, ^{13}CNMR and FTIR spectra; (Figs. S6, S7) Melting and crystallization DSC curves; (Figs. S8-S11) TGA and DTGA curves in air; (Figs. S12-S15) TGA and DTGA curves in nitrogen.

Appendix A. Supporting information

Supplementary data associated with this article can be found in the online version at doi:10.1016/j.mtcomm.2022.103469.

References

[1] G. Scott, in: G. Scott (Ed.), Oxidation and stabilisation of polymers during processing. In Atmospheric oxidation and antioxidants, Vol.II, Elsevier, Amsterdam, 1993, pp. 141–218.
[2] G. Scott, in: G. Scott (Ed.), Photodegradation and photostabilisation. In Atmospheric oxidation and antioxidants, Vol.II, Elsevier, Amsterdam, 1993, pp. 385–430.
[3] N.C. Billingham, in: G. Scott (Ed.), The physical chemistry of polymer oxidation and stabilization. In Atmospheric oxidation and antioxidants, Vol.II, Elsevier, Amsterdam, 1993, pp. 219–278.
[4] G. Scott, in: G. Scott (Ed.), Macromolecular and polymer-bound antioxidants. In Atmospheric oxidation and antioxidants, Vol.II, Elsevier, Amsterdam, 1993, pp. 279–326.
[5] G. Kasza, K. Mosnáčková, A. Nádor, Z. Osváth, T. Stumphauser, G. Szarka, K. Czaniková, J. Rychlý, S. Chmela, B. Iván, J. Mosnáček, Synthesis of hyperbranched poly(ethyleneimine) based macromolecular antioxidants and investigation of their efficiency in stabilization of polyolefins, Eur. Polym. J. 68 (2015) 609–617.
[6] S. Beer, I. Teasdale, O. Brueggemann, Immobilization of antioxidants via ADMET polymerization for enhanced long-term stabilization of polyolefins, Eur. Polym. J. 49 (2013) 4257–4264.
[7] S. Losio, I. Tritto, L. Boggion, G. Mancini, G. Luciano, L. Tofani, C. Viglianisi, S. Menichetti, M.C. Sacchi, P. Stagnaro. Fully consistent terpolymeric non-releasing antioxidant additives for long lasting polyolefin packaging materials, Polym. Deg. Stab. 144 (2017) 167–175.
[8] G. Zhang, H. Li, M. Antensteiner, T.C.M. Chung, Synthesis of functional polypropylene containing hindered phenol stabilizers and applications in metallized polymer film capacitors, Macromolecules 48 (2015) 2925–2934.
[9] M. Yuan, G. Zhang, B. Li, T.C.M. Chung, R. Rajagopalan, M.T. Lanagan, Thermally stable low-loss polymer dielectrics enabled by attaching cross-linkable antioxidant to polypropylene, ACS Appl. Mater. Interfaces 12 (2020) 14154–14164.
[10] T.C.M. Chung, Expanding polyethylene and polypropylene applications to high-energy areas by applying polyolefin-bonded antioxidants, Macromolecules 52 (2019) 5618–5637.
[11] G. Zhang, C. Nam, L. Petersson, J. Jämbeck, H. Hillborg, T.C.M. Chung, Increasing polypropylene high temperature stability by blending polypropylene-bonded hindered phenol antioxidant, Macromolecules 51 (2018) 1927–1936.
[12] G. Zhang, C. Nam, T.C.M. Chung, Polypropylene copolymer containing cross-linkable antioxidant moieties with long-term stability under elevated temperature conditions, Macromolecules 50 (2017) 7041–7051.
[13] L.S. Boffa, B.M. Novak, Copolymerization of polar monomers with olefins using transition-metal complexes, Chem. Rev. 100 (2000) 1479–1493.
[14] N.M.G. Franssen, J.N.H. Reek, B. de Bruin, Synthesis of functional 'polyolefins': state of the art and remaining challenges, Chem. Soc. Rev. 42 (2013) 5809–5832.
[15] A. Martín, M. Hoyos, J.M. Gómez-Elvira, Exploring functionalities for the development of high thermal stability polypropylene-based dielectrics, ACS Appl. Energy Mater. 4 (2021) 25–29.
[16] R. Krache, R. Benavente, J.M. López-Majada, J.M. Pereña, M.L. Cerrada, E. Pérez. α, β, and γ polymorphs in a β-nucleated metallocenic isotactic polypropylene, Macromolecules 40 (2007) 6871–6878.
[17] U.M. Stehling, K.M. Stein, M.R. Kesti, R. M. Waymouth. Metallocene/borate-catalyzed polymerization of amino-functionalized R-olefins, Macromolecules 31 (1998) 2019–2027.
[18] M.J. Schneider, R. Schäfer, R. Mülhaupt, Arninofunctional linear low density polyethylene via metallocene-catalysed ethene copolymerization with N,N-bis (trimethylsilyl)-1-amino-10-undecene, Polymer 38 (1997) 2455–2459.

[19] J. Huang, G.L. Rempel, Ziegler-natta catalysts for olefin polymerization: mechanistic insights from metallocene systems, Prog. Polym. Sci. 20 (1995) 459–526.
[20] R.J. Gritter, R.J. Chriss, Free-radical reactions of pyrroles, J. Org. Chem. 29 (1964) 1163–1167.
[21] T. Usami, S. Takayama, Fine-branching structure in high-pressure, low-density polyethylenes by 50.10-MHz carbon-13 NMR analysis, Macromolecules 17 (1984) 1756–1761.
[22] J. Chen, A. Motta, B. Wang, Y. Gao, T.J. Marks, Significant polar comonomer enchainment in zirconium-catalyzed, masking reagent-free, ethylene copolymerizations, Angew. Chem. Int. Ed. 58 (2019) 7030–7034.
[23] J. Chen, A. Motta, B. Wang, Y. Gao, T.J. Marks, Angew. Chem. 131 (2019) 7104–7108.
[24] M.R. Radlauer, A.K. Buckley, L.M. Henling, T. Agapie, Bimetallic coordination insertion polymerization of unprotected polar monomers: copolymerization of amino olefins and ethylene by dinickel bisphenoxyiminato catalysts, J. Am. Chem. Soc. 135 (2013) 3784–3787.
[25] L. Resconi, I. Camurati, O. Sudmeijer, Chain Transf. React. Propyl. Polym. zirconocene Catal. Top. Catal. 7 (1999) 145–163.
[26] A. Carvill, L. Zetta, G. Zannoni, M.C. Sacchi, ansa-zirconocene-catalyzed solution polymerization of propene: influence of polymerization conditions on the unsaturated chain-end groups, Macromolecules 31 (1998) 3783–3789.
[27] M. Huang, J. Chen, B. Wang, W. Huang, H. Chen, Y. Gao, T. J. Marks. Polar isotactic and syndiotactic polypropylenes by organozirconium-catalyzed masking-reagent-free propylene and amino–olefin copolymerization, Angew. Chem. 132 (2020) 20703–20709.
[28] I.A. Jacobson Jr, H.H. Heady, G.U. Dinneen, Thermal reactions of organic nitrogen compounds, I. 1-methylpyrrole. J. Phys. Chem. 62 (1958) 1563–1565.
[29] I.A. Jacobson, H.B. Jensen, Thermal reactions of organic nitrogen compounds. II. 1-n-butylpyrrole, J. Phys. Chem. 66 (1962) 1245–1247.
[30] I.A. Jacobson, H.B. Jensen, Thermal reactions of organic nitrogen compounds. III. 1-Isopropylpyrrole, J. Phys. Chem. 68 (1964) 3068–3070.
[31] Data Organic Chemistry, Reich Collection, ⟨https://organicchemistrydata.org/hansreich/resources/nmr/?index=nmr_index%2F13C_shift#cdata185⟩.